MNRAS **000**, 000–000 (0000) Preprint 11 January 2019 Compiled using MNRAS LATEX style file v3.0

Merging black hole binaries with the SEVN code

Mario Spera[1,2,3,4,5,6]★, Michela Mapelli[1,2,3,4]†, Nicola Giacobbo[1,2,3], Alessandro A. Trani[3,7,8], Alessandro Bressan[3,8], and Guglielmo Costa[8]
[1] *Dipartimento di Fisica e Astronomia 'G. Galilei', University of Padova, Vicolo dell'Osservatorio 3, I–35122, Padova, Italy*
[2] *INFN, Sezione di Padova, Via Marzolo 8, I–35131, Padova, Italy*
[3] *INAF, Osservatorio Astronomico di Padova, Vicolo dell'Osservatorio 5, I–35122, Padova, Italy*
[4] *Institut für Astro- und Teilchenphysik, Universität Innsbruck, Technikerstrasse 25/8, A-6020, Innsbruck, Austria*
[5] *Department of Physics and Astronomy, Northwestern University, Evanston, IL 60208, USA*
[6] *Center for Interdisciplinary Exploration and Research in Astrophysics (CIERA), Evanston, IL 60208, USA*
[7] *Department of Astronomy, Graduate School of Science, The University of Tokyo, 7-3-1 Hongo, Bunkyo-ku, Tokyo, 113-0033, Japan*
[8] *SISSA, via Bonomea 265, I-34136 Trieste, Italy*

11 January 2019

APPENDIX A: INTERPOLATION

A1 Single stars

To evolve a star s with ZAMS mass $M_{\rm ZAMS,s}$ and metallicity Z_s at time t, in SEVN we use four interpolation tracks from the look-up tables. Two of them have metallicity $Z_1 = Z_s - \Delta Z$ and ZAMS masses $M_{\rm ZAMS,1} = M_{\rm ZAMS,s} - \Delta M$ and $M_{\rm ZAMS,2} = M_{\rm ZAMS,s} + \Delta M$, respectively, where ΔM is the step of the mass grid of the look-up tables at metallicity Z_1 and ΔZ is the step of the metallicity of the look-up tables. The other two interpolation tracks have ZAMS masses $M_{\rm ZAMS,1}$ and $M_{\rm ZAMS,2}$ and metallicity $Z_2 = Z_s + \Delta Z$. To begin with, we calculate the percentage of life $\Theta_{\rm p}$ of the star s on its macro-phase p (see equation 1). Then, we use the interpolation tracks to calculate

$$M_{s,Z_j}(t) = \beta_1 M_{1,Z_j}\left(t_{1,Z_j}\right) + \beta_2 M_{2,Z_j}\left(t_{2,Z_j}\right) \tag{A1}$$

where

$$t_{i,Z_j} \equiv \Theta_{\rm p}\left(t_{\rm f,p,i,Z_j} - t_{0,\rm p,i,Z_j}\right) + t_{0,\rm p,i,Z_j}, \tag{A2}$$

$$\beta_1 \equiv \frac{M_{\rm ZAMS,1}\left(M_{\rm ZAMS,2} - M_{\rm ZAMS,s}\right)}{M_{\rm ZAMS,s}\left(M_{\rm ZAMS,2} - M_{\rm ZAMS,1}\right)}, \tag{A3}$$

$$\beta_2 \equiv \frac{M_{\rm ZAMS,2}\left(M_{\rm ZAMS,s} - M_{\rm ZAMS,1}\right)}{M_{\rm ZAMS,s}\left(M_{\rm ZAMS,2} - M_{\rm ZAMS,1}\right)}, \tag{A4}$$

$i, j \in [1, 2]$ and $t_{0,\rm p,i,Z_j}$ $\left(t_{\rm f,p,i,Z_j}\right)$ is the starting (end) time of the macro-phase p of the star with ZAMS mass M_i at metallicity Z_j.

The use of the β_1 and β_2 weights allows us to keep the interpolation error below 1% with respect to the original PARSEC evolutionary tracks and to include less points in the look-up tables. We refer to Spera & Mapelli (2017) for more details on the weights. We calculate the interpolated value of the mass of the star s at time t as

$$M_s(t) = \gamma_1 M_{s,Z_1}(t) + \gamma_2 M_{s,Z_2}(t), \tag{A5}$$

where $\gamma_1 \equiv \frac{Z_s - Z_1}{Z_2 - Z_1}$ and $\gamma_2 \equiv \frac{Z_2 - Z_s}{Z_2 - Z_1}$.

A2 Binary stars

Every time a star has accreted (donated) a significant amount of mass Δm from (to) its companion, the code looks for new interpolation tracks in the look-up tables. We avoid to jump to new tracks when Δm is small, thus we impose that a change of track can occur only if $\Delta m > \gamma_m M$, where M is the total mass of the star, γ_m is a parameter with typical value of ~ 0.01, and Δm is the mass exchange (loss or gain). The rules governing a change of track depend primarily on the star's macro-phase.

Hereafter, we call *old star* the star that is still on the old track while we use *new star* to refer to the star that has moved to a new track.

A2.1 Stars in the H phase

To change the evolutionary track for stars in the H phase we require that the new star has the same percentage of life ($\Theta_{\rm H}$) and the same total mass of the old star. We define

$$\Theta_{\rm H} \equiv \frac{t_{\rm loc}}{t_{\rm HeS}}, \tag{A6}$$

where $t_{\rm loc}$ is the time on the stellar track and $t_{\rm HeS}$ is the starting time of the He phase. We also check that

$$\frac{|M_1 - M_0|}{M_0} < \epsilon_1, \tag{A7}$$

where M_1 is the mass of the new star, M_0 is the mass of the old star, and ϵ_1 is a parameter with a typical value of $\sim 10^{-3}$. To find the new track we implemented an iterative algorithm. We assume that the new track will not be far from the one with

$$M_{\rm ZAMS,new} = M_{\rm ZAMS,old} \pm \Delta m. \tag{A8}$$

The sign in the above equation is $-$ ($+$) if the star is a donor (accretor).

Thus, we choose the interval $M_{\rm ZAMS} \in$

$\left[M_{\rm ZAMS,1}, M_{\rm ZAMS,2}\right]$ as the fiducial range to find the new stellar track, where

$$M_{\rm ZAMS,1} = M_{\rm ZAMS,old} \pm \xi_{\rm low}\Delta m, \tag{A9}$$

$$M_{\rm ZAMS,2} = M_{\rm ZAMS,old} \pm \xi_{\rm high}\Delta m. \tag{A10}$$

The values of the parameters $\xi_{\rm low}$ and $\xi_{\rm high}$ are chosen by experiment and have typical values of ~ 0.2 and ~ 1.2, respectively. As starting values, the algorithm evaluates the mass of the star at times $t_1 = p\, t_{\rm HeS,1}$ and $t_2 = p\, t_{\rm HeS,2}$, where the subscripts 1 and 2 refer to the tracks with ZAMS masses $M_{\rm ZAMS,1}$ and $M_{\rm ZAMS,2}$, respectively. The next iterations are given by

$$M_0 - m\left(t_{n-1}\right) = \frac{m\left(t_n\right) - m\left(t_{n-1}\right)}{M_{\rm ZAMS,}n - M_{\rm ZAMS,}n-1} \times \left(M_{\rm ZAMS,}n+1 - M_{\rm ZAMS,}n-1\right), \tag{A11}$$

where $n = 0, 1, 2..., n_{\rm max}$, $M_{\rm ZAMS,}n+1$ is the ZAMS mass of the new candidate track and $m\left(t_n\right)$ is the mass of the star at time t_n (here n is the number of iterations). The algorithm stops if equation (A7), with $M_1 = m\left(t_{n+1}\right)$, is verified or, in any case, if $M_{\rm ZAMS,}n+1$ goes beyond the tracks included in the look-up tables, or if a maximum of $n_{\rm max}$ = `MAX_iterations_H` iterations is reached. The default value of the `MAX_iterations_H` parameter is 8. If the condition (A7) is never verified, the new track will be the one with the minimum value of $\frac{|M_1 - M_0|}{M_0}$.

A2.2 Stars in the He phase

For this category we need to distinguish stars that have a Hydrogen envelope from WR stars.

i) To change track for WR stars, we use the look-up tables of bare Helium cores (see Sec. 2.1.2). To find a new track we use the same algorithm described for the stars in the H phase, with the following appropriate changes: $M_{\rm ZAMS} \rightarrow M_{\rm He-ZAMS}$, $\Theta_{\rm H} \rightarrow \Theta_{\rm He} \equiv \frac{t_{\rm loc}}{t_{\rm COS}}$, where $t_{\rm COS}$ is the time when the CO core starts to decouple from Helium.

ii) A new track for He stars with a Hydrogen envelope is successfully found if the following conditions are simultaneously verified

$$\frac{\left|M_{\rm He,1} - M_{\rm He,0}\right|}{M_{\rm He,0}} < \epsilon_2, \tag{A12}$$

$$\frac{|M_1 - M_0|}{M_0} < \epsilon_3, \tag{A13}$$

where $M_{\rm He,1}$ is the mass of the He core of the new star, $M_{\rm He,0}$ is the mass of the He core of the old star, and ϵ_2 and ϵ_3 are two parameters with a typical value of $\sim 10^{-3}$ and $\sim 10^{-2}$, respectively. The algorithm starts to inspect the track with ZAMS mass given by equation (A9) and the ZAMS is changed iteratively with a mass step $\Delta m = \pm 0.2$. Here, we adopt the minus sign for a donor star (in this case we check for a new track with $M_{\rm ZAMS} < M_{\rm ZAMS,0}$) and the plus sign for an accretor (in this case we check for a new track with $M_{\rm ZAMS} > M_{\rm ZAMS,0}$). The new star is searched in the time interval $\left[t_{0,\rm He}, t_{\rm f,He}\right]$. If both the conditions (A12) and (A13) are verified, a new track is found, otherwise the algorithm does not change the track.

A2.3 Stars in the CO phase

In this case we use an algorithm analogous to that described for He stars (see section A2.2). The difference is that for stars in the CO phase we search the new track in the time interval $\left[t_{0,\rm CO}, t_{\rm SN}\right]$ where $t_{0,\rm CO}$ is the time when the CO core starts to decouple from Helium and $t_{\rm SN}$ is the time when the star transforms into a compact remnant. If the star is a WR, we search the new track in the time interval $\left[\max\left(t_{0,\rm CO}, t_{\rm He,max}\right), t_{\rm SN}\right]$.

A3 The temporal evolution of a star

To evolve the mass of a star from time t_1 to time $t_2 = t_1 + \Delta t$, we use the formula

$$M_2 = M_1 + V_m\, M_1, \quad \text{where } V_m = \frac{m_2 - m_1}{m_1}. \tag{A14}$$

In the above formula M_2 is the mass of the star at time t_2, M_1 is the mass of the star at time t_1, m_1 and m_2 are the masses of the star obtained from the interpolation tracks at time t_1 and t_2, respectively (see Equation A1), and V_m is the relative variation of the mass of the star, calculated from the interpolation tracks. We use equation A14 because, should the track-finding algorithm not converge (i.e. $|m_1 - M_1| > \epsilon_1 M_1$, see equation A7), the temporal evolution of M is still continuous.

In contrast, if the track-finding algorithm converges, we have $M_1 \simeq m_1$, that is $M_2 \simeq m_2$, which means that the evolution of the star is synchronous with the values in the look-up tables. We adopt the same technique for the temporal evolution of $M_{\rm He}$, and $M_{\rm CO}$, while we keep R, L and time always synchronous with the values obtained with the interpolation tracks.

APPENDIX B: PRESCRIPTIONS FOR SNE

Uncertainties on models of core-collapse SNe are still large (see Foglizzo et al. 2015 for a recent review). Overall, there is consensus that the properties of the progenitor star at the onset of core collapse determine the mass of the compact remnant, but the details differ significantly from one model to the other. For this reason, in SEVN we decided to implement several different models, which can be activated with a different option in the parameter file. The models currently available in SEVN are the following:

- The delayed core-collapse model is described in Fryer et al. (2012) and in Spera et al. (2015). It is based on the calculations by Fryer et al. (2012) and on the idea that the shock is launched > 0.5 s after the onset of core collapse. In this model, the final mass of the remnant depends just on the mass of the CO core and on the final mass of the star (i.e. the total mass before the onset of core collapse).
- The rapid core-collapse model is also described in Fryer et al. (2012) and in Spera et al. (2015). The only difference

between the rapid and the delayed SN model is the time when the shock is launched: < 250 ms after the onset of core collapse in the case of the rapid SN model. Both the delayed and the rapid model depend only on the mass of the CO core and on the final mass of the progenitor star.

- The STARTRACK model is the same as adopted in the STARTRACK code (Belczynski et al. 2010). Also in this case, the mass of the final remnant depends only on the CO core mass and on the final mass of the star. The final remnant masses are similar to the ones obtained with the rapid model.
- The compactness model is based on the compactness of the stellar interior at the onset of core collapse, defined as (O'Connor & Ott 2011)

$$\xi_{2.5} = \frac{2.5\,\mathrm{M}_\odot}{R(2.5\,\mathrm{M}_\odot)/\mathrm{km}}, \tag{B1}$$

which is the measure of a characteristic mass (in this case $2.5\,\mathrm{M}_\odot$) divided by the radius which encloses this mass at the onset of core collapse. Previous work (O'Connor & Ott 2011; Ugliano et al. 2012; Horiuchi et al. 2014) shows that if $\xi_{2.5} \gtrsim 0.2$ a star is expected to directly collapse to a BH. Unlike the former three models, the model based on the compactness requires that we know the internal properties of a star at the onset of collapse, when a Fe core is already formed. Thus, this model cannot be used self-consistently in combination with stellar-evolution models that do not describe nuclear burning up to the formation of a Fe core.
- The two-parameter model is based on the mass for which the dimensionless entropy per nucleon is $s = 4$ (M_4) and on the mass gradient at the same location ($\mu_4 = dM/dr|_{s=4}$). Ertl et al. (2016) have proposed this model, based on the fact that the complex physics of core-collapse SNe cannot be described entirely by a single parameter like the compactness. The underlying idea is that μ_4 scales with the ram-pressure on the infalling material from the outer layers of the collapsing star, while $M_4\,\mu_4$ scales with the neutrino luminosity. As for the compactness, also the two-parameter model requires that we know the internal properties of a star at the onset of core collapse.

The first three models we described (delayed, rapid and STARTRACK) depend only on the CO core mass and on the final mass of a star, while the latter two models depend on the internal structure of a star at the onset of core collapse. The latter models are more accurate but require modelling the interior structure of a star at the onset of core collapse. Recently, Limongi (2017) and Limongi & Chieffi (2018) have shown that there is a strong correlation between the CO core mass and the compactness at the onset of core collapse, suggesting that even the more approximated models capture the main features of core collapse.

Unlike core-collapse SNe, the physical mechanisms powering PISNe have been understood and satisfactorily described (Ober et al. 1983; Bond et al. 1984; Heger et al. 2003; Woosley et al. 2007). In very massive, metal-poor stars the central temperature can rise above $\sim 7 \times 10^8$ K, leading to an effective production of positron and electron pairs. This removes radiation pressure, causing the core to contract. The result is an increase of the central temperature, leading to an early and simultaneous switching on of Oxygen and Silicon burning. If $64 \lesssim M_{\rm He}/\mathrm{M}_\odot \lesssim 135$ (where $M_{\rm He}$ is the Helium core mass) the star is completely destroyed by the explosive burning of Oxygen and Silicon (Woosley 2017), leaving no compact remnant. This mechanism is known as PISN. If $M_{\rm He} > 135\ \mathrm{M}_\odot$, the early contraction of the core cannot be stopped and the star collapses to a BH directly. If $32 \lesssim M_{\rm He}/\mathrm{M}_\odot \lesssim 64$, the stellar core can undergo one or more oscillations, during which mass loss is significantly enhanced. This mechanism is known as pulsational PISN (PPISN, Woosley 2017). At the end of the oscillations, the star finds a new equilibrium and dies with a core-collapse SN. As described in Spera & Mapelli (2017), we have included both PISNe and PPISNe in SEVN, following the models of Woosley (2017). In particular, the mass of the remnant is described as

$$m_{\rm rem,PISN} = f(M_{\rm He},\, m_{\rm fin})\, m_{\rm rem,noPISN}, \tag{B2}$$

where $m_{\rm rem,PISN}$ ($m_{\rm rem,noPISN}$) is the final mass of the compact remnant when we account (we do not account) for PISNe and PPISNe, while $f(M_{\rm He},\, m_{\rm fin})$ is a function of the Helium core mass and of the final mass of the star, described in Appendix B of Spera & Mapelli (2017).

Another issue related to SNe is the natal kick of the compact remnant. There are no direct measurements of the natal kick of BHs, but only indirect studies based on the proper motion of few X-ray binaries (Gualandris et al. 2005; Fragos et al. 2009; Repetto et al. 2012, 2017). As for neutron stars (NSs), Hobbs et al. (2005) have derived the proper motions of 233 isolated pulsars in the Milky Way, showing that their distribution can be fit with a Maxwellian distribution with one-dimensional root-mean square $\sigma_{\rm kick} = 265$ km s^{-1}. This result is still debated (e.g. Faucher-Giguère & Kaspi 2006; Verbunt et al. 2017), especially for binary NSs (Beniamini & Piran 2016; Beniamini et al. 2016; Giacobbo & Mapelli 2018), but is still the most used distribution for natal kicks of NSs.

In SEVN, we adopt the Hobbs et al. (2005) kick distribution for both NSs and BHs but we scale it by the amount of fallback (Fryer et al. 2012):

$$V_{\rm kick} = (1 - f_{\rm fb})\, W_{\rm kick}, \tag{B3}$$

where $f_{\rm fb}$ is the fallback factor (the explicit expression can be found in Giacobbo et al. 2018), and $W_{\rm kick}$ is randomly drawn from the Maxwellian distribution derived by Hobbs et al. (2005). According to this formalism, if a BH forms by prompt collapse of the parent star $V_{\rm kick} = 0$.

If the SN occurs when the BH or NS progenitor is member of a binary, the SN kick can unbind the system. The survival of the binary system depends on the orbital elements at the moment of the explosion and on the SN kick. If the binary remains bound, its post-SN semi-major axis and eccentricity are calculated as described in appendix A1 of Hurley et al. (2002).

APPENDIX C: MASS TRANSFER

C1 Wind mass transfer

The mean accretion rate by stellar winds is calculated as (Bondi & Hoyle 1944, see also eq. 6 of Hurley et al. 2002)

$$\langle \dot{M}_2 \rangle = \frac{1}{\sqrt{1-e^2}} \left(\frac{G\,M_2}{v_{\rm W}^2} \right)^2 \frac{\alpha_{\rm W}}{2\,a^2} \frac{1}{(1+v^2)^{3/2}}\, \dot{M}_1, \tag{C1}$$

where $\dot{M}_1$ is the mass lost by the donor by stellar winds ($\dot{M}_1 > 0$), M_2 is the accretor mass, e is the orbital eccentricity, G is the gravitational constant, a is the semi-major axis, and $\alpha_W = 1.5$ (Hurley et al. 2002), while v and v_W are defined as follows:

$$v^2 = \frac{G\,(M_1 + M_2)}{a\,v_W^2}, \tag{C2}$$

$$v_W^2 = 2\,\beta_W \left(\frac{G\,M_1}{R_1}\right), \tag{C3}$$

where M_1 is the mass of the donor, R_1 is the radius of the donor and the dimensionless parameter $\beta_W \sim 0.1-7$ depends on the spectral type (Hurley et al. 2002). $\langle \dot{M}_2 \rangle$ in equation C1 is averaged over an orbital period and is strictly valid only if $v_W >> G\,(M_1 + M_2)/a$. We impose that $\dot{M}_2 \leq 0.8\,|\dot{M}_1|$ to avoid that more mass is accreted by the secondary than is lost by the primary, under some special circumstances.

Non-conservative mass transfer also induces a change in the angular momentum of the system. Following Hurley et al. (2002), we describe the orbit-averaged change of angular momentum due to wind mass transfer as

$$\dot{J}_{orb} = \left(\dot{M}_1\,M_2 - M_1\,\dot{M}_2\right)\,M_2\,(1-e^2)^{1/2}\left[\frac{G\,a}{(M_1+M_2)^3}\right]^{1/2} \tag{C4}$$

In equation C4, we assume that only the primary loses mass and only the secondary accretes mass, which is not true in the general case, because both stars lose mass by stellar winds. If we assume that both binary members donate and accrete mass at the same time, equation C4 is generalized as

$$\dot{J}_{orb} = \left[\left(\dot{M}_{1L}\,M_2 - M_1\,\dot{M}_{2A}\right)\,M_2 + \left(\dot{M}_{2L}\,M_1 - M_2\,\dot{M}_{1A}\right)\,M_1\right] (1-e^2)^{1/2}\left[\frac{G\,a}{(M_1+M_2)^3}\right]^{1/2}, \tag{C5}$$

where $\dot{M}_{1L}$ and $\dot{M}_{1A}$ ($\dot{M}_{2L}$ and $\dot{M}_{2A}$) are the mass loss rate and the mass accretion rate of the primary (secondary), respectively[1].

Non-conservative wind mass transfer also affects the spins of the stars. The change of the spin angular momentum of the primary due to stellar winds is described as (Hurley et al. 2002)

$$\dot{J}_{spin,1} = -\frac{2}{3}\dot{M}_{1L}\,R_1^2\,J_{spin,1}\,I_1^{-1} + \frac{2}{3}\dot{M}_{1A}\,R_2^2\,J_{spin,2}\,I_2^{-1}, \tag{C6}$$

where $\dot{M}_{1L}$ is the mass loss rate by stellar winds of the primary, $\dot{M}_{1A}$ is the mass accretion rate by wind accretion of the primary, $J_{spin,1}$ ($J_{spin,2}$) is the spin angular momentum of the primary (secondary) and I_1 (I_2) is the inertia of the primary (secondary). The change of the spin angular momentum of the secondary is described in the same way, by changing the subscripts accordingly.

Following Hurley et al. (2002), the orbit-averaged change of eccentricity is

$$\frac{\dot{e}}{e} = -\dot{M}_2\left(\frac{1}{M_1+M_2} + \frac{1}{2\,M_2}\right), \tag{C7}$$

where $\dot{M}_2$ is the mass accretion rate averaged over a time-step.

[1] The sign of equations C4 and C5 is different from the one reported by Hurley et al. (2002) only because in our formalism the mass loss rate is positive $\dot{M}_{1L} > 0$, $\dot{M}_{2L} > 0$.

C2 Roche-lobe overflow

At every time-step we evaluate whether one of the two members of the binary fills its Roche lobe by using equation 6 (Eggleton 1983).

If the Roche-lobe filling donor is a neutron star (NS, $k = 13$) or a BH ($k = 14$), the accretor must be another NS or BH. In this case, the two objects are always merged. In all the other cases, to decide the amount of mass transferred from the primary Δm_1, we first evaluate the stability of mass transfer using the radius-mass exponents ζ defined by Webbink (1985). In particular, $\zeta_{ad} \equiv \frac{d\ln R_1}{d\ln m_1}|_{ad}$ is the change of radius of the donor needed to reach a new hydrostatic equilibrium as a consequence of mass loss, $\zeta_{th} \equiv \frac{d\ln R_1}{d\ln M_1}|_{th}$ is the change of radius of the donor needed to reach a new thermal equilibrium as a consequence of mass loss, and $\zeta_L \equiv \frac{d\ln R_{L,1}}{dM_1}$ is the change of the Roche lobe induced by mass loss. ζ_{ad}, ζ_{th} and ζ_L are calculated as described in Hurley et al. (2002).

Following Hurley et al. (2002) we do not estimate ζ_{ad} directly, but we adopt a simplified criterion: we use the critical mass ratio q_c defined as the mass ratio for which $\zeta_{ad} = \zeta_L$ (Soberman et al. 1997). Following BSE,

$$q_c = \begin{cases} 0.695 & \text{if } k = 0 \\ 3 & \text{if } k = 1,4 \\ 4 & \text{if } k = 2 \\ 0.362 + 1.0\,\left[3.0\,(1.0 - M_{c,1}/M_1)\right]^{-1} & \text{if } k = 3,5,6 \\ 0.784 & \text{if } k = 8,9 \\ 0.628 & \text{if } k = 10,11,12 \end{cases} \tag{C8}$$

where $M_{c,1}$ is the mass of the core of the donor[2].

If the Roche-lobe filling donor is a first giant branch star (type $k = 3$) or a core Helium burning (cHeB) star ($k = 4$) or an asymptotic giant branch (AGB) star ($k = 5,6$) or an Hertzsprung gap (HG) Naked Helium star ($k = 8$) or a Giant Branch Naked Helium star ($k = 9$), we start a CE phase if $q_1 > q_C$.

If a deeply convective MS star (mass < 0.7 M$_\odot$, $k = 0$) fills its Roche lobe and $q_1 > q_c$, the two stars are merged. The mass accreted by the merger product is decided as in Hurley et al. (2002).

If both the donor and the accretor are MS stars with mass > 0.7 M$_\odot$ ($k = 1$) or HG stars ($k = 2$) and $q_1 > q_c$, we always merge them (note that Hurley et al. (2002) allow HG stars to enter CE rather than being merged if $q_1 > q_c$).

If the donor is a WD ($k = 10, 11, 12$) and $q_1 > q_c$, the two stars are merged. The treatment of the merger product is the same as described in Hurley et al. (2002). The formalism based on q_c contains several simplifications. In the future updates of SEVN we will include a more accurate formalism.

If $\zeta_L > \zeta_{ad}$, mass transfer is unstable over a dynamical timescale (i.e. the radius of the primary increases faster than the Roche lobe on conservative mass transfer). If this condition is satisfied when the donor is a MS or a HG star, the binary is merged. If this condition is satisfied by any other non-degenerate donor, the binary enters a CE phase.

[2] Up-to-date values for ζ_{ad} and q_c can be found in Claeys et al. (2014) and in Ge et al. (2015), respectively. We will include the new values in the next version of the SEVN code

If $\zeta_L < (\zeta_{ad}, \zeta_{th})$ mass transfer is stable, until nuclear evolution changes the radius of the star. In this case, the mass loss rate of the primary is described by equation 7.

If $\zeta_{th} < \zeta_L < \zeta_{ad}$, mass transfer is unstable on a thermal timescale. Equation 7 can be considered an upper limit to mass loss in this case, because the thermal timescale is small compared to the nuclear timescale. We thus calculate the mass loss as the minimum between the values given in equation 7 and 8.

The accreted mass Δm_2 in the case of a stable mass transfer or of a thermally unstable mass transfer is described by equation 9 if the accretor is not a compact object, and by equation 10 if the accretor is a compact object.

If the accretor is a WD we also consider the possibility of a nova eruption. In particular, if the donor is Hydrogen rich ($k \leq 6$) and $\dot{M}_1 < 1.03{\times}10^{-7}$ M$_\odot$ yr^{-1}, we assume that a nova occurs and the accreted matter is only $\Delta m_{2,\rm nova} = f_{\rm nova}\,\Delta m_2$, where $f_{\rm nova} = 0.001$ (Hurley et al. 2002).

Non-conservative mass transfer also affects the orbital angular momentum of the system and the spins of the star. The variation of orbital angular momentum is described as

$$\dot{J}_{\rm orb} = (\dot{M}_1 - \dot{M}_2)\, M_2^2\, (1-e^2)^{1/2} \left[\frac{G\,a}{(M_1+M_2)^3}\right]^{1/2} \quad \text{(C9)}$$

In this equation, we assume that the material lost from the system carries with it the specific angular momentum of the primary.

If the accretion onto a compact object is super-Eddington or if there is a nova eruption, we use a different prescription for the variation of the orbital angular momentum:

$$\dot{J}_{\rm orb} = (\dot{M}_1 - \dot{M}_2)\, M_1^2\, (1-e^2)^{1/2} \left[\frac{G\,a}{(M_1+M_2)^3}\right]^{1/2}, \quad \text{(C10)}$$

which means that we assume that this mass is lost by the system as a wind from the secondary.

The loss of spin angular momentum of the primary by Roche lobe overflow is described as

$$\dot{J}_{\rm spin,1} = \dot{M}_1\, R_{\rm L,1}^2\, J_{\rm spin,1}\, I_1^{-1}, \quad \text{(C11)}$$

where $R_{\rm L,1}$ is the Roche lobe of the primary, while $J_{\rm spin,1}$ and I_1 are the spin angular momentum and the inertia of the primary (i.e. the Roche lobe filling star).

The spin up of the secondary (i.e. the accretor) depends on whether an accretion disc forms around it. According to BSE, the accretion disc radius is estimated as (Ulrich & Burger 1976)

$$R_{\rm D} = 0.0425\,{\rm R}_\odot\, a\, [q_2\,(1+q_2)]^{1/4} \quad \text{(C12)}$$

If $R_{\rm D} > R_2$, then a disc forms and the change of spin angular momentum of the secondary is

$$\dot{J}_{\rm spin,2} = \dot{M}_2\, (G\, M_2\, R_{\rm L,2})^{1/2}, \quad \text{(C13)}$$

where $R_{\rm L,2}$ is the Roche lobe of the accretor. Here we assume that material falls onto the star from the inner edge of a Keplerian accretion disc and that the system is in a steady state.

If $R_{\rm D} \leq R_2$, then we calculate the change of spin as

$$\dot{J}_{\rm spin,2} = \dot{M}_2\, (G\, M_2\, 1.7\, R_{\rm D})^{1/2}. \quad \text{(C14)}$$

This results in a spin up of the accretor. We then check if the final spin is larger than the critical spin (above which the star is expected to break up)

$$J_{\rm crit} = I_2 \left(\frac{2}{3}\right)^{3/2} \left[\frac{G\,(M_2+\Delta m_2)}{R_2^3}\right]^{1/2}, \quad \text{(C15)}$$

where I_2 is the inertia of the accretor.

If $(J_{\rm spin,2} + \dot{J}_{\rm spin,2}\, dt) > J_{\rm crit}$, we force the final spin of the accretor to be the same as $J_{\rm crit}$. It is not clear whether stars can keep accreting once they reach the break-up spin (see Packet 1981, Popham & Narayan 1991, Petrovic et al. 2005, de Mink et al. 2013). Here we assume that viscous coupling with the circumstellar disk can efficiently remove angular momentum from the star without halting the accretion flow.

APPENDIX D: SUPPLEMENTARY FIGURES

In this appendix we show the masses of merging compact-object binaries (Fig. D1), the distribution of chirp masses of merging BHBs (Fig. D2) and the distribution of the mass ratio of merging BHBs (Fig. D3) for all the considered metallicities ($Z \in [10^{-4}; 4\times10^{-2}]$).

REFERENCES

Belczynski K., Bulik T., Fryer C. L., Ruiter A., Valsecchi F., Vink J. S., Hurley J. R., 2010, ApJ, 714, 1217
Beniamini P., Piran T., 2016, MNRAS, 456, 4089
Beniamini P., Hotokezaka K., Piran T., 2016, ApJ, 829, L13
Bond J. R., Arnett W. D., Carr B. J., 1984, ApJ, 280, 825
Bondi H., Hoyle F., 1944, MNRAS, 104, 273
Claeys J. S. W., Pols O. R., Izzard R. G., Vink J., Verbunt F. W. M., 2014, A&A, 563, A83
Eggleton P. P., 1983, ApJ, 268, 368
Ertl T., Janka H.-T., Woosley S. E., Sukhbold T., Ugliano M., 2016, ApJ, 818, 124
Faucher-Giguère C.-A., Kaspi V. M., 2006, ApJ, 643, 332
Foglizzo T., et al., 2015, Publ. Astron. Soc. Australia, 32, e009
Fragos T., Willems B., Kalogera V., Ivanova N., Rockefeller G., Fryer C. L., Young P. A., 2009, ApJ, 697, 1057
Fryer C. L., Belczynski K., Wiktorowicz G., Dominik M., Kalogera V., Holz D. E., 2012, ApJ, 749, 91
Ge H., Webbink R. F., Chen X., Han Z., 2015, ApJ, 812, 40
Giacobbo N., Mapelli M., 2018, preprint, (arXiv:1805.11100)
Giacobbo N., Mapelli M., Spera M., 2018, MNRAS, 474, 2959
Gualandris A., Colpi M., Portegies Zwart S., Possenti A., 2005, ApJ, 618, 845
Heger A., Fryer C. L., Woosley S. E., Langer N., Hartmann D. H., 2003, ApJ, 591, 288
Hobbs G., Lorimer D. R., Lyne A. G., Kramer M., 2005, MNRAS, 360, 974
Horiuchi S., Nakamura K., Takiwaki T., Kotake K., Tanaka M., 2014, MNRAS, 445, L99
Hurley J. R., Tout C. A., Pols O. R., 2002, MNRAS, 329, 8 97
Limongi M., 2017, preprint, (arXiv:1706.01913)
Limongi M., Chieffi A., 2018, ApJS, 237, 13
O'Connor E., Ott C. D., 2011, ApJ, 730, 70
Ober W. W., El Eid M. F., Fricke K. J., 1983, A&A, 119, 61
Packet W., 1981, A&A, 102, 17
Petrovic J., Langer N., van der Hucht K. A., 2005, A&A, 435, 1013
Popham R., Narayan R., 1991, ApJ, 370, 604
Repetto S., Davies M. B., Sigurdsson S., 2012, MNRAS, 425, 2799
Repetto S., Igoshev A. P., Nelemans G., 2017, MNRAS, 467, 298

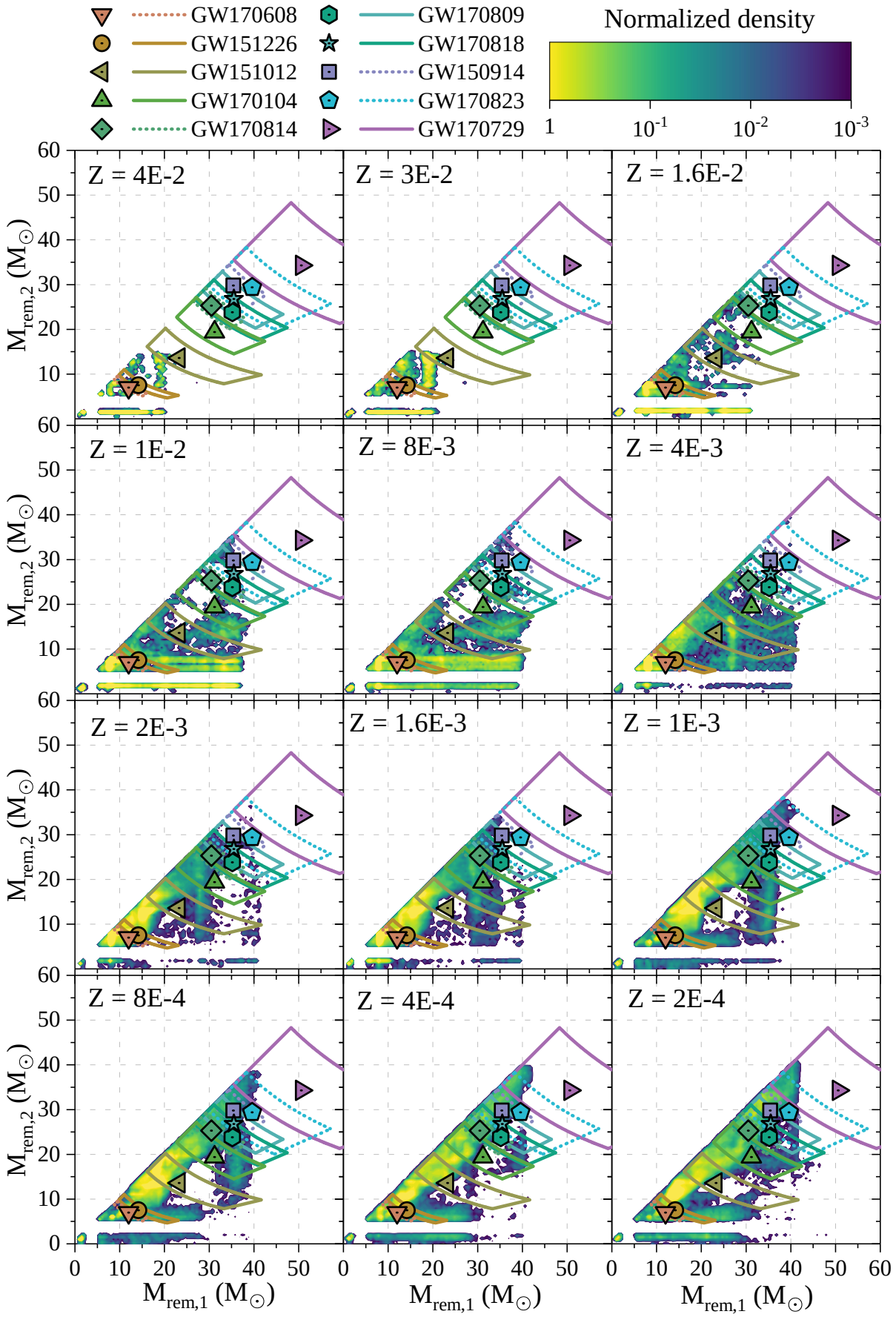

Figure D1. Same as the panels in the bottom row of Fig. 6, but for all the other metallicities considered in our simulations.

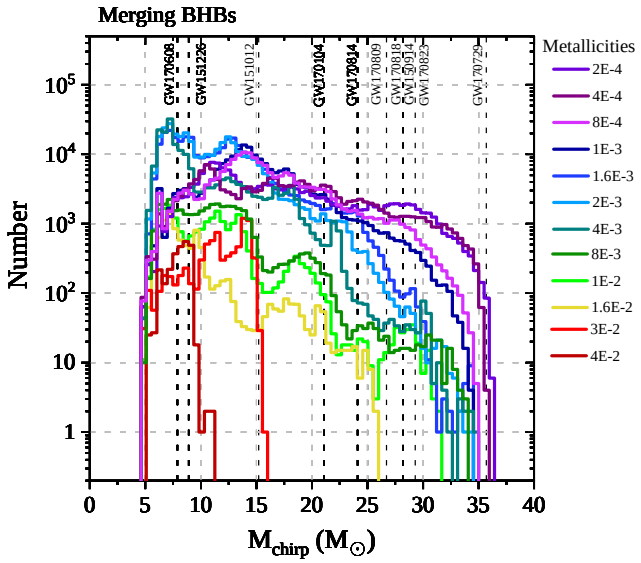

Figure D2. Same as Fig. 7, but for all the considered metallicities.

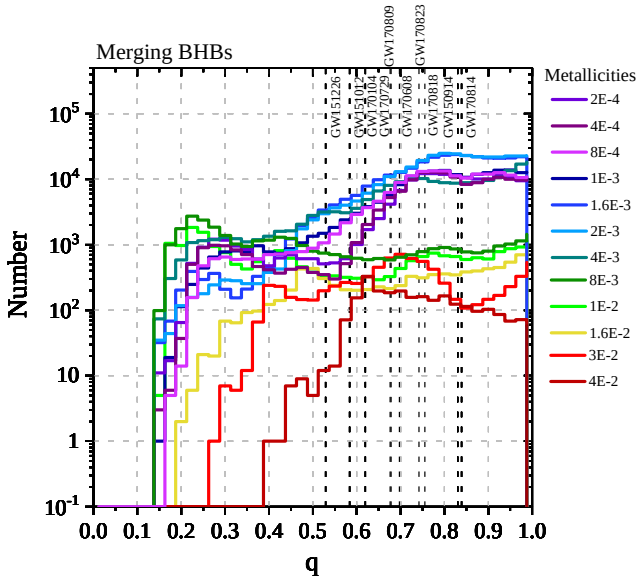

Figure D3. Same as Fig. 8, but for all the considered metallicities.

Soberman G. E., Phinney E. S., van den Heuvel E. P. J., 1997, A&A, 327, 620
Spera M., Mapelli M., 2017, MNRAS, 470, 4739
Spera M., Mapelli M., Bressan A., 2015, MNRAS, 451, 4086
Ugliano M., Janka H.-T., Marek A., Arcones A., 2012, ApJ, 757, 69
Ulrich R. K., Burger H. L., 1976, ApJ, 206, 509
Verbunt F., Igoshev A., Cator E., 2017, A&A, 608, A57
Webbink R. F., 1985, Stellar evolution and binaries. p. 39
Woosley S. E., 2017, preprint, (arXiv:1608.08939)
Woosley S. E., Blinnikov S., Heger A., 2007, Nature, 450, 390
de Mink S. E., Langer N., Izzard R. G., Sana H., de Koter A., 2013, ApJ, 764, 166